Quadrature Signal Generator with Improved DC Offset Compensation

Djordje STOJIC
Electrical Institute Nikola Tesla, Koste Glavinica 8a, 11000 Belgrade, Serbia
djordje.stojic@ieent.org

***Abstract*—In this paper a second order generalized integrator (SOGI) based quadrature signal generator (QSG) is proposed with the improved DC offset compensation parameter tuning procedure. Namely, for the conventional DC rejection technique, which comprises an integrator (I) included in the SOGI, the modified parameter tuning procedure is proposed based on the set QSG response damping factor value. In this way, when compared to existing QSG tuning techniques based on empirical trial-and-error approach, simplified parameter tuning procedure is proposed based on proposed parametric equations, which enable improved QSG performance verified by simulation and experimental runs by a single-phase phase-locked loop PLL. In this way the increased SOGI based QSG DC offset compensation speed can be achieved, which is critical in various types of single phase PLL applications.**

***Index Terms*—estimation, frequency locked loops, nonlinear control systems, phase locked loops, power conversion.**

I. Introduction

The DC offset component in the PLL input represents a major problem in the synchronization and regulation of the grid-connected power converters, electrical machines, power quality measurement and various other applications [1-3]. Causes of the DC component can be different—offset in the voltage sensors and A/D conversion, grid faults, semiconductor device mismatches [1], DC injection from the distributed power generation utilities [3], etc. The DC offset in the PLL input results in the low frequency oscillations at the estimated quantities, which are difficult to remove without significantly deteriorating the PLL dynamic performance. The DC offset should preferably be removed before it enters the PLL, by processing the PLL input signals.

The DC offset compensation may differ in the three [4] and single phase PLL applications [5], because the single-phase PLL applications require QSG [6], and that the DC offset compensation needs to be included in the QSG [7]. Different approaches are proposed for the DC offset compensation in the literature for single and three phase applications. The primary focus of this paper is on the single-phase applications.

The principal task in the single phase PLL applications is QSG, which can be performed by various means [5-6]. The QSG, which is frequently used in the literature, represents the SOGI based solution [8-10], a conventional algorithm that belongs to the wider group of the adaptive filter based PLL applications [11]. One of the major problems related to the SOGI based QSG is the propagation of the DC offset from the input to the output. When SOGI is applied in a PLL, the DC offset causes an AC component in the estimated frequency and phase angle values, which needs to be removed. This is performed by various DC offset compensation techniques proposed in the literature.

In a previous research [1], a comprehensive review is presented, which includes experimental comparison and verification of conventional DC offset compensation techniques in QSG, that are mainly based on the SOGI adaptive filters. The algorithm proposed in another study [2] represents a commonly used modification of SOGI, which comprises the integrator term introduced to compensate the DC offset at the SOGI input. However, although the proposed technique successfully removes the DC offset at the SOGI output, the integral term introduction significantly deteriorates the resulting QSG dynamic performance.

In another previous study [12], an intrinsic SOGI feature is exploited that enables DC offset compensation by combining the corresponding internal SOGI signals. However, the problem with this approach is that the employed internal SOGI filter contains highly amplified high frequency noise, which results in the inaccurate QSG, and consequently in the erroneous frequency and phase angle estimation in the following PLL. As a result, to improve the findings of the previous study mentioned in [12], the low-pass filter (LPF) is introduced to reduce the high frequency content in the internal SOGI signal used for the DC offset compensation [13].

In research [14], two cascaded SOGI are used to remove the DC offset from the generated quadrature component, which results in the QSG with the reduced response times. Finally, in the previous study mentioned in [7], the least mean square (LMS) based adaptive filter is proposed to compensate the DC offset at the QSG input, having the problem related to the high computational load required by the LMS based algorithm.

In this paper, the new parameter tuning procedure for the SOGI based QSG is proposed, with the DC offset compensation tuning based on the modification of the algorithm proposed in a previous research [2]. Instead of tuning the SOGI closed-loop poles to have the same real parts as in the study [2], the novel parameter tuning procedure is proposed, in which a real pole and pair of conjugate-complex poles—that make up the three SOGI closed-loop poles—all have the same pole frequency. In this way, a simplified and improved DC offset compensation is achieved in SOGI, which is proven in the paper by analytical means, and also, by the simulation and experimental test runs. Consequently, the main contribution outlined in this paper regarding existing solutions comprises

This work was supported in part by the Serbian Ministry of Science by institutional funding.

Digital Object Identifier 10.4316/AECE.2021.03008

1582-7445 © 2021 AECE

the modified pole-placement technique of the closed-loop poles of the SOGI based single-phase PLL with input DC offset compensation, which results in modified PLL parameter tuning procedure and in the improved PLL dynamic performance characteristics.

This paper consists of seven sections. In section II, three conventional SOGI based QSG are presented, which include the DC offset compensation. In section III, the novel DC compensation is presented, based on the modification of the QSG proposed in the previous study mentioned in [1]. In section IV, the novel QSG parameter tuning procedure is presented. In section V, the simulation results are presented, while in section VI, the experimental results are outlined.

II. The Conventional DC Offset Compensation Techniques for SOGI Based QSG

The SOGI based QSG represents one of the conventional solutions widely used in practice [1], which is represented in Fig. 1.

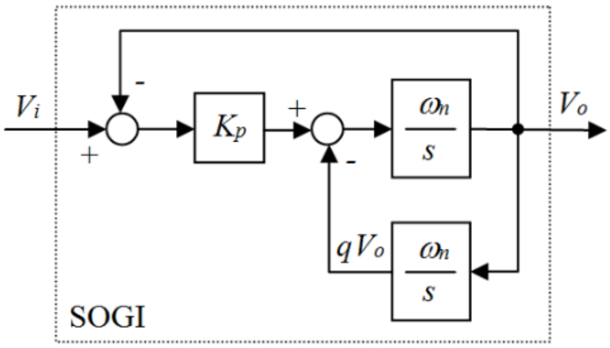

Figure 1. The SOGI based QSG

In Fig. 1, the signal V_i represents the SOGI input, V_o denotes the direct SOGI output component in the phase with the V_i, while qV_o represents the quadrature SOGI output that is orthogonal to the input signal V_i. Furthermore, K_p represents the SOGI filter parameter, while ω_n represents the angular frequency of the SOGI input signal V_i.

In the following equations, the corresponding SOGI transfer functions are outlined, illustrating the direct and quadrature signal generation and filtering of SOGI features.

$$G_{Vo}(s) = \frac{V_o(s)}{V_i(s)} = \frac{K_p \omega_n s}{s^2 + K_p \omega_n s + \omega_n^2} \tag{1}$$

$$G_{qVo}(s) = \frac{qV_o(s)}{V_i(s)} = \frac{K_p \omega_n^2}{s^2 + K_p \omega_n s + \omega_n^2} \tag{2}$$

By analysing equations (1) and (2), it can be concluded that in steady-state (for s=$j\omega_n$), $V_o(j\omega_n)$ = $V_i(j\omega_n)$, while $qV_o(j\omega_n)$ is orthogonal to $V_o(j\omega_n)$, i.e. $qV_o(j\omega_n) = V_i(j\omega_n)/j = V_i(j\omega_n)\text{e-}j\pi/2$. Also, based on equations (1) and (2), it can be concluded that the SOGI serves as the band-pass filter in case (1), and as the LPF in case (2).

Regarding the DC offset propagated from the SOGI input, it can be concluded that the DC offset is filtered out from the V_o because of presence of the differential terms in the numerator of Equation (1). However, the DC offset is propagated from the SOGI input to the qV_o output, amplified by factor K_p, which represents one of the main SOGI shortcomings, discussed in a previous study [1].

To compensate the DC offset in SOGI QSG, the following three techniques are proposed in the literature.

A. The SOGI Expanded with an Integral Term

In the previous study mentioned in [2], a commonly used DC offset compensation technique is presented, which includes an integral term (I) in the ISOGI, illustrated in Fig. 2.

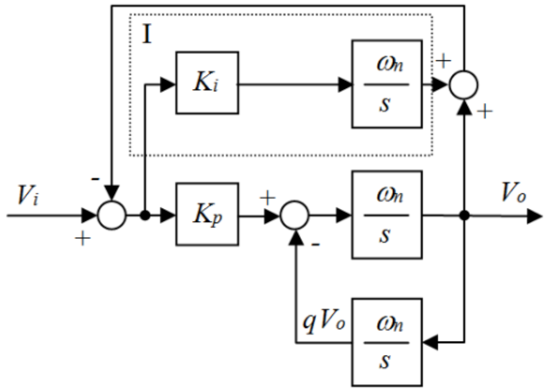

Figure 2. The ISOGI

The ISOGI outlined in Fig. 2 successfully compensates the DC offset, which is analysed in the study mentioned in [2]. However, the problem with structure in Fig. 2 is that, it is difficult to set the SOGI parameters K_i and K_p to get QSG dynamic performance comparable with those achieved by a conventional SOGI from Fig. 1. This is analysed in section III. Concerning solution [2], the improvement proposed in the new solution comprises the modifications introduced in the closed-loop pole placement technique of the resulting single-phase PLL based on the ISOGI QSG outlined in the Fig. 2.

B. The Double SOGI (DSOGI)

The second conventional technique used for the DC offset compensation in SOGI based QSG is based on the utilisation of two SOGI blocks in series, outlined in Fig. 3.

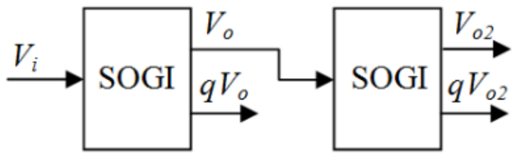

Figure 3.The DSOGI

In Fig. 3, V_i, V_o and qV_o represent signals typical for SOGI structure in Fig. 1, while V_{o2} and qV_{o2} represent direct and quadrature output signal of DSOGI for the input V_i.

Based on equations (1) and (2), the following DSOGI transfer functions (3) and (4) are got.

$$G_{Vo2}(s) = \frac{V_{o2}(s)}{V_i(s)} = G_{Vo}(s)\ G_{Vo}(s) \tag{3}$$

$$G_{qVo2}(s) = \frac{V_{qo2}(s)}{V_i(s)} = G_{Vo}(s)\ G_{qVo}(s) \tag{4}$$

From equations (1) and (2), it can be concluded that in steady-state, V_{o2} is in phase with V_i, qV_{o2} is orthogonal to V_i, while the DC offset is filtered out from both V_{o2} and qV_{o2}. However, introducing the second SOGI in DSOGI, also introduces the additional time lag in the proposed QSG response time, making it slower when compared to the original SOGI. Also, DSOGI is more complex to implement when compared to ISOGI. Consequently, regarding DSOGI based solutions, the novel SOGI based parameter tuning procedure introduces improvements in the resulting single-phase PLL dynamic performance, which are outlined by following simulation and experimental test results, and simplifies resulting QSG stage implementation.

C. The Low-pass Filter Based DC Offset Compensation

In the two previous studies [12-13], the LPF based DC offset compensation in SOGI based QSG is proposed, outlined in Fig. 4.

Namely, in the study mentioned in [12], it is shown that in steady-state, V_1 signal has the same DC component as qV_o, while it also contains significantly amplified high frequency noise component from V_i. The signal V_1 is filtered by LPF and subtracted from qV_o to get qV_{lpf}, which is orthogonal to V_i and free from high frequency noise component [13].

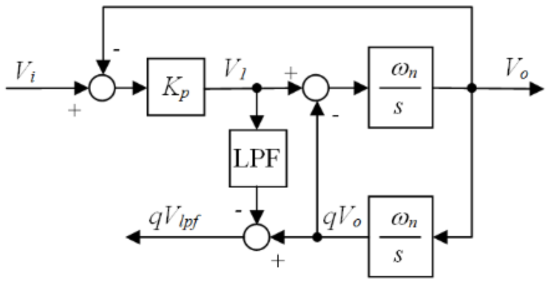

Figure 4. The LPF based DC offset compensation in SOGI

However, the shortcoming of the method proposed in the previous study [13] is that significant low-pass filtration is required, because V_i is commonly contaminated with high frequency components, which results in the reduced QSG response times. Also, SOGI with LPF is more complex to implement in relation to the ISOGI. Regarding LPF based SOGI, the novel solution introduces improved resulting PLL dynamic performance, outlined in following simulation and experimental test results, and it simplifies the implementation of the resulting single-phase PLL with input signal DC offset compensation.

In the following section, the ISOGI based QSG is proposed, with the modified parameter tuning procedure.

III. MODIFIED ISOGI PARAMETER TUNING PROCEDURE

The new ISOGI parameter tuning procedure is based on the closed-loop transfer function derived by using the ISOGI open-loop transfer function $W_{ISOGI}(s)$, outlined in Equation (5).

$$W_{isogi}(s) = K_p \frac{\omega_n s}{s^2+\omega_n^2} + K_i \frac{\omega_n}{s} = K_p \left[\frac{s^2\left(K_p\omega_n + K_i\right) + K_i\omega_n^3}{K_p s\left(s^2+\omega_n^2\right)} \right] \tag{5}$$

Based on Equation (5), the closed-loop ISOGI transfer function (6) is derived.

$$G_{isogi}(s) = \frac{W_{isogi}(s)}{1+W_{isogi}(s)} = \frac{\omega_n\left[s^2\left(K_p+K_i\right)+K_i\omega_n^2\right]}{s^3+s^2\left(K_p+K_i\right)\omega_n+s\omega_n^2+K_i\omega_n^3} \tag{6}$$

The dynamic analysis of ISOGI is performed by analysing the roots of the $G_{isogi}(s)$ characteristic polynomial, the denominator in transfer function (6) and $D_{isogi}(s)$ in Equation (7).

$$D_{isogi}(s) = s^3 + s^2\left(K_p+K_i\right)\omega_n + s\omega_n^2 + K_i\omega_n^3 \tag{7}$$

In the study mentioned in [2], the tuning procedure of the parameters K_p and K_i is proposed, which is improved by the new procedure proposed in this paper.

A. The ISOGI Parameter Tuning Procedure in [2]

In the study mentioned in [2], the closed-loop ISOGI poles, calculated by Equation (7), are tuned by choosing K_p and K_i values, to get the one real pair of conjugate-complex poles, where all have the same real part α_p. The corresponding characteristic polynomial (8) is got, where β_p represents the imaginary part of the resulting conjugate-complex poles.

$$D_{isogi}(s) = \left(s+\alpha_p\right)\left(s+\alpha_p+j\beta_p\right)\left(s+\alpha_p-j\beta_p\right) \tag{8}$$

From Equation (7), the following Equation (9) is got, which determines the relation between K_p and K_i, to get the closed-loop ISOGI poles that have the same real part, as in Equation (8).

$$K_i^3 + 3K_pK_i^2 + \left(3K_p^2+9\right)K_i + K_p^3 - 4.5K_p = 0 \tag{9}$$

The equation (9) represents the final instruction proposed in the study mentioned in [2]: how to choose K_p and K_i, where K_i needs to be calculated by Equation (9) for empirically chosen K_p. The range for $K_p \in [0.5,1.5]$ is suggested, which should, according to [2], enable the preferable ISOGI dynamic performance. Finally, the ISOGI parameter tuning procedure [2] (although it is significantly based on the empirical tuning) represents the most comprehensive ISOGI tuning procedure that can be found in the literature.

Hence, in this paper, an improved ISOGI parameter tuning procedure is presented, which is not based on an empirical trial-and-error based procedure as outlined in [2]; but rather requires only one design criterion to be defined as input procedure parameter—the required ISOGI closed-loop conjugate-complex poles dumping factor ζ_p. For example, the value of $\zeta_p \in [0.6, 0.8]$ is suggested for the damping factor value of the dominant closed-loop system conjugate-complex poles [15] in control systems.

B. Novel ISOGI Parameter Tuning Procedure

In the novel parameter tuning procedure (contrary to the idea used in [2], in which the resulting closed-loop ISOGI poles have the same real part), the underlying idea is to get the closed-loop poles, in which all have the same natural frequency ω_p, with the conjugate-complex pair of poles having the damping factor ζ_p. The underlying idea is to examine could a novel approach to the choice of the QSG closed-loop poles (the same poles real parts in [2] compared to the same poles natural frequency in this paper) yield increased QSG response speeds for the similar overshot values, including maximum allowable. The following characteristic polynomial (10) is attained.

$$D_{isogi}(s) = \left(s+\omega_p\right)\left(s^2+2\zeta_p\omega_p s+\omega_p^2\right) \tag{10}$$

Based on equations (7) and (10), the following equations (11) and (12) are derived for ISOGI parameters K_p and K_i.

$$K_i = \left(2\zeta_p+1\right)^{-3/2} \tag{11}$$

$$K_p = 4\,\zeta_p\left(\zeta_p+1\right)\left(2\zeta_p+1\right)^{-3/2} \tag{12}$$

By analysing equations (11) and (12), it can be concluded that the new parameter tuning procedure represents a straightforward link between the required ISOGI dominant conjugate-complex closed-loop poles damping factor ζ_p and the values of parameters K_i and K_p. This represents a significant improvement and simplification, when compared to the parameter tuning procedure outlined in [2], where K_i and K_p are tuned by empirical, trial-and-error procedure, in which ISOGI dynamic performance is examined for each empirically chosen value K_p, and for the corresponding K_i value calculated from K_p by Equation (9).

In the new parameter tuning procedure, for K_i and K_p values calculated by equations (11) and (12), the following ω_p value is got, as described in Equation (13).

$$\omega_p = \frac{\omega_n}{\sqrt{2\zeta_p + 1}} \tag{13}$$

Consequently, the main objective of the novel ISOGI based single-phase parameter tuning procedure is to attain the designated value of the closed-loop conjugate-complex poles dumping factor ζ_p, which results in PLL parameters calculated by (11) and (12), and resulting PLL closed-loop poles natural frequency ω_p (13) (which corresponds to the resulting PLL bandwidth frequency value).

In the following section, the simulation results are presented for all the existing QSG algorithms with DC offset compensation that are outlined in section II. These results are compared with the simulation results of the ISOGI with the new improved parameter tuning procedure.

IV. Simulation Runs

In this section, the results of the simulation tests are presented and compared between the existing [1], [16-25] and new QSG techniques with the compensated DC offset.

A. Simulation Tests of DSOGI

The DSOGI in Fig. 3 represents two SOGI blocks in series, where for each of SOGI blocks parameter, the value K_p needs to be tuned. For the rated input signal angular frequency ω_p = 2π50 rad/s and $K_p \in [1, 2]$, the following simulation responses are presented in Fig. 5, which represent the amplitude voltage V_{amp} of the estimated orthogonal system of voltages V_o and qV_o.

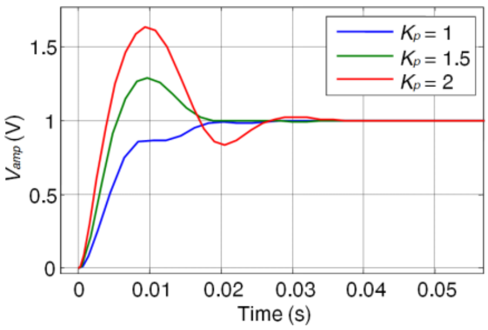

Figure 5. The DSOGI V_{amp} signal simulation results for three different K_p values

By analysing the simulation results in Fig. 5, it can be concluded that the increase in K_p value causes the increase in the DSOGI response overshoot and settling time. Finally, for K_p = 1, the DSOGI response with no overshoot is got with rising time t_r = 13 ms and settling time t_{set} = 18 ms.

B. Simulation of LPF Based DC Offset Compensation

In two previous studies [12-13], the influence of the LPF bandwidth and order on the SOGI response is presented, showing that the decrease in LPF bandwidth causes the deterioration in the SOGI dynamic performance. However, the decrease in the LPF bandwidth is usually required, because the signal V1, in Fig. 4, commonly contains significant high frequency noise contents. In Fig. 6, the Vamp simulation results are presented for SOGI in Fig. 4, for the first order LPF (which according to [12-13] represents the best case scenario regarding the resulting SOGI dynamic performance) and for three different bandwidth (BW) values. Also, the simulation results are presented for the rated input signal angular frequency value ω_n = 2π50 rad/s, where in the studies [12-13] the LPF BW does not exceed the SOGI input signal ω_n value.

By analysing V_{amp} responses in Fig. 7, it can be concluded that the best ISOGI performance is obtained for K_p = 1. Namely, for K_p = 0.5, the rising time is significantly decreased, while for K_p = 1.5, although the fastest rising time is got, the settling time is increased when compared to the responses got for K_p = 1. For the ISOGI with preferable dynamic performance for K_p = 1, the following response parameters are got: t_r = 14 ms, settling time t_{set} = 32 ms and overshoot O_s = 20%.

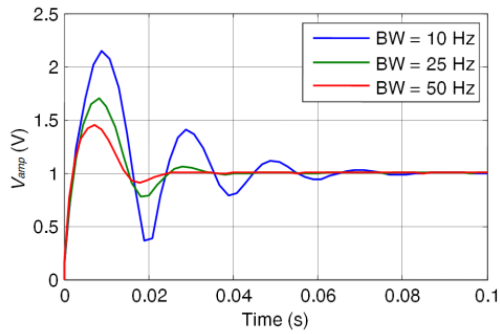

Figure 6. Simulation results of V_{amp}, for SOGI with LPF, for three different LPF BW values

C. Simulation Results for the ISOGI with the Parameter Tuning Procedure Outlined in [2]

In the previous research stated in [2], an empirical parameter tuning procedure is proposed, based on the trial-and-error choice of the K_p value, and on the corresponding K_i value calculated by Equation (9). The ISOGI is simulated for the rated input signal angular frequency value ω_n = 2π50 rad/s and for the range of K_p values suggested in the study mentioned in [2] ($K_p \in [0.5, 1.5]$), with the corresponding results presented in Fig. 7.

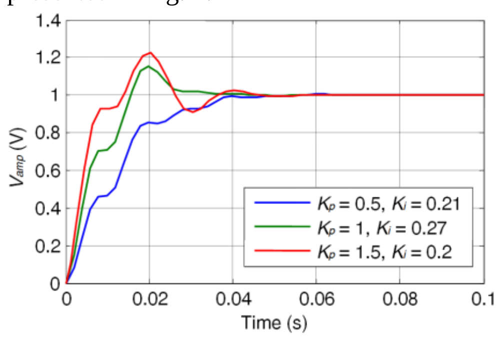

Figure 7. The V_{amp} simulation responses for ISOGI tuned by the procedure outlined in [2], for three different values of K_p parameter and for corresponding K_i values calculated by Equation (9)

D. Simulation Results for the ISOGI with the New Parameter Tuning Procedure

In equations (11) and (12), the new ISOGI parameter tuning procedure is provided for the required dominant poles damping factor ζ_p. In Fig. 8, V_{amp} responses are presented for values of K_p and K_i parameters calculated for three different ζ_p values.

Here is the list of ISOGI parameters that correspond to a particular ζ_p value: (i) for ζ_p = 0.6, K_p = 1.17 and K_i = 0.3, (ii) for ζ_p = 0.7, K_p = 1.28 and K_i = 0.27 and (iii) for ζ_p = 0.8, K_p = 1.37 and K_i = 0.24 are got. By analysing responses in Fig. 8, the best response is got for ζ_p = 0.7, where the following V_{amp} response parameters are obtained: t_r = 11 ms, settling time t_{set} = 25 ms and overshoot O_s = 22%. In this way, the QSG parameter tuning procedure can completely be defined.

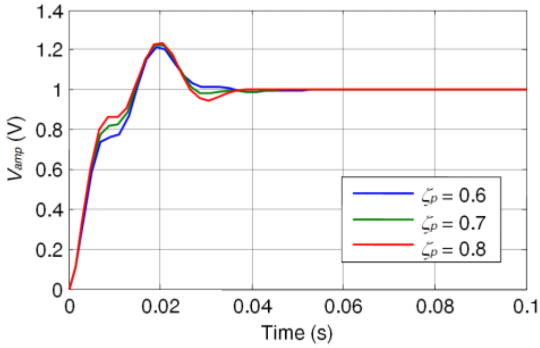

Figure 8. The ISOGI V_{amp} signal responses for the new parameter tuning procedure applied for three different damping factor values ζ_p

E. Comparison of the Simulation Results Between the Presented four Different DC Offset Compensation Techniques

By analysing the best case responses in the previous subsections, the following conclusions can be made:

The DSOGI responses from subsection A provide the best compromise between overshoot and rising and settling times. However, the DSOGI represents the most complex algorithm for the practical implementation.

The LPF based SOGI from subsection B exhibits notable increases in overshoot and settling time with the decrease in the LPF bandwidth.

When comparing the new ISOGI parameter's tuning procedure with the procedure outlined in [2], it can be concluded that the new one provides faster response and settling times with the similar overshoot values. However, while the new method establishes the direct tuning method determined by the required ISOGI dominant poles damping factor ζ_p, the parameter tuning procedure in [2] is based on the trial-and-error parameter tuning, where the K_i values are calculated by Equation (9) for empirically chosen K_p value. This confirms that the idea behind the novel parameter tuning procedure yielded satisfactory results, since faster QSG responses are got when compared with [2], for similar overshot values, including maximum allowable. Also, if smaller overshoots are required, in the new procedure corresponding damping factor ζ_p could be chosen, while in [2] this could be achieved by a corresponding empirical trial-and-error method.

In the following section, the frequency responses of four QSG algorithms previously analysed in Section IV are presented to illustrate and compare their filtering capabilities.

V. QSG Frequency Responses

In this section, the frequency responses are analysed and compared for different QSG implementations. This is necessary, because in QSG, the input signal filtration is required, especially for the higher order harmonics, which are typically present in the grid voltage measurements, which are used in the single phase PLL applications.

By analysing the frequency responses in Fig. 9, it can be concluded that DSOGI introduces -20 dB/dec attenuation at the V_{o2} output and -40 dB/dec attenuation at qV_{o2}, which is typical for the SOGI applications with the DC offset compensation [1].

By analysing the frequency response in Fig. 10, it can be concluded that SOGI with LPF based DC offset compensation introduces an attenuation of -20 dB/dec at both V_o and qV_o outputs, which results in the reduced filtration of the higher order harmonics, when compared with DSOGI.

By analysing frequency responses in Fig. 11, it can be concluded that the higher order harmonics filtration, similar to DSOGI, is achieved: -20 dB/dec attenuation at V_o and -40 db/dec at qV_o outputs.

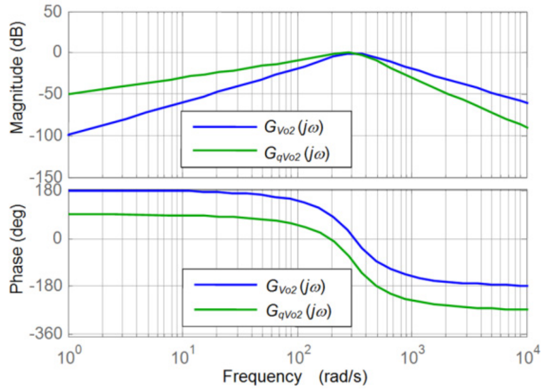

Figure 9. Frequency responses of the DSOGI QSG from Fig. 3, for K_p = 1 and $\omega_n = 2\pi50$ rad/s

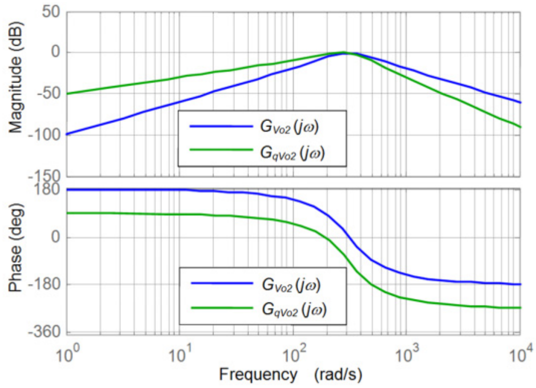

Figure 10. Frequency responses of the SOGI with LPF from Fig. 4, for LPF BW = 50 Hz and $\omega_n = 2\pi50$ rad/s

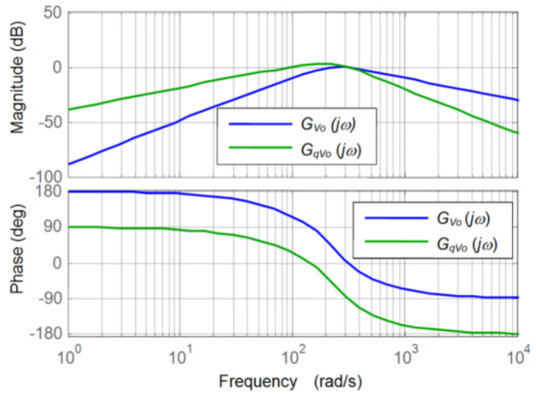

Figure 11. Frequency responses for ISOGI from Fig. 2, tuned by the procedure outlined in study [2] with K_p = 1, K_i = 0.27 and $\omega_n = 2\pi50$ rad/s

By analysing frequency responses in Fig. 12, it can be concluded that the ISOGI tuned by the new procedure enables the same level of higher order harmonics filtration, similar to the DSOGI and ISOGI tuned by using the procedure outlined in the previous study [2]: -20 dB/dec attenuation at V_o and -40 db/dec at qV_o outputs. However, as it is shown in section IV that the novel parameter tuning procedure enables faster ISOGI responses, when compared to the procedure outlined in [2], while ISOGI is less complex to implement when compared to DSOGI.

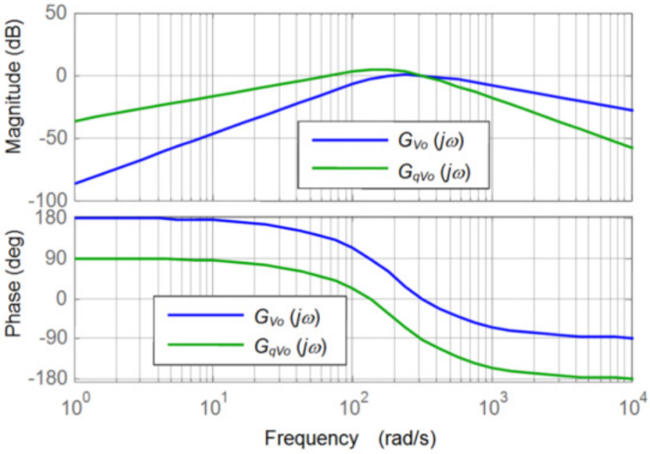

Figure 12. Frequency responses of ISOGI tuned by the new procedure, with K_p = 1.28, K_i = 0.27 and $\omega_n = 2\pi 50$ rad/s

In the following section VI, the results of experimental tests are presented.

VI. EXPERIMENTAL TESTS

In this section, the results of the experimental tests are presented. Namely, four different QSG algorithms with the DC offset compensation are tested by a digital signal processor based platform, used for the single phase synchronisation of a grid-connected power converter. The power grid synchronisation unit is based on the TMS320F28335 microcontroller, while the power grid voltage is emulated by a programmable signal generator.

A. Estimated Orthogonal Voltage System Amplitude Vamp for the Input Signal DC Offset Variations

In Fig. 13, the experimental results are presented for four different QSG algorithms with DC offset compensation. The input voltage amplitude is calculated for the DC offset 0.5 V, introduced in the input signal.

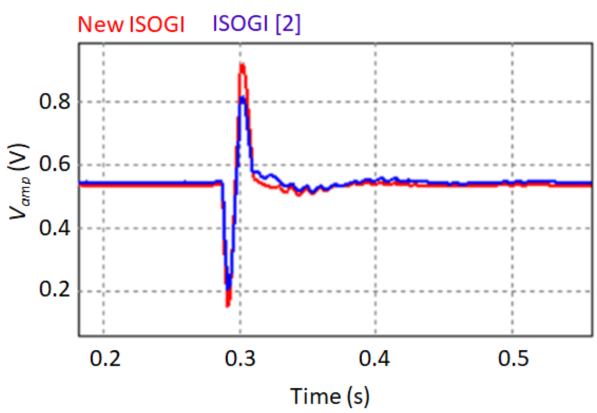

(a)

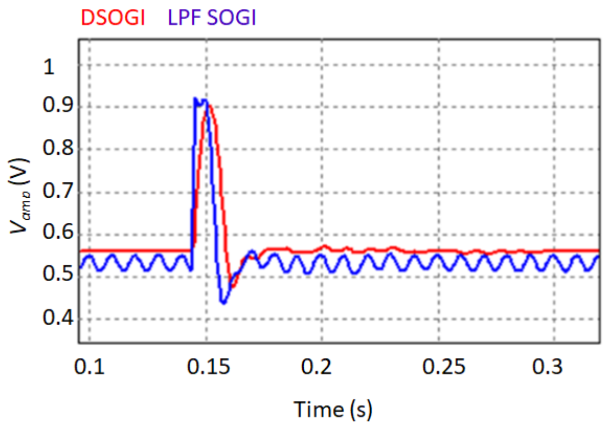

(b)

Figure 13. The V_{amp} response for (a) ISOGI tuned by using new procedure and the procedure outlined in a previous study [2], and (b) for DSOGI and SOGI with LPF

By analysing responses in Fig. 13, the following QSG settling times are obtained: (i) for ISOGI tuned by new procedure with K_p = 1.28 and K_i = 0.27, the time is t_{set} = 25 ms, (ii) for ISOGI tuned by using a procedure outlined in the previous study [2] with K_p = 1 and K_i = 0.27, the time is t_{set} = 40 ms, (iii) for DSOGI with K_s = 1.5, the time is t_{set} = 30 ms, and (iv) for SOGI with LPF with K_s = 2 and LPF BW = 50 Hz, the time is t_{set} = 30 ms. Based on the presented results, it can be concluded that the new ISOGI parameter tuning procedure enables the fastest QSG response times.

B. Phase-locked Loop for Four Different QSG Algorithms for the Input Signal DC Offset Variations

In this subsection, the comparison is presented for four QSG methods with input DC offset compensation, used in the conventional PLL scheme [1] in Fig. 14. In this scheme, frequency adaptive filtering is used in the QSG PLL stage, meaning that the frequency estimate ω_{est} is fed into the QSG stage by equating the QSG parameter ω_n with ω_{est}, i.e., by using $\omega_n = \omega_{est}$ in the QSG stage. This is, also, shown in the Fig. 14.

In Fig. 14, the signals V_α and V_β represent the QSG estimated outputs for the input signal V_i, V_d and V_q denote the PLL rotational frame components, ω_{ff} is the feed-forward value for the estimated frequency component (that is commonly set at the rated input signal frequency value, which is for power converters connected to European power grid typically set at the value $\omega_{ff} = 2\pi 50$ rad/s), ω_{est} represent the estimated frequency value and θ_{est} denote the estimated phase angle value. The PLL parameter K_{ppll} and K_{ipll} values are calculated by using the symmetrical optimum method, which is employed in [1]. The symmetrical optimum method is defined by the required PLL phase margin PM, which is used to calculate the following parameter b value (14). In this paper, extended symmetrical optimum method is used, proposed in [26], and, also, employed in [27].

The PLL crossover frequency ω_c is calculated by using the value of b, the OQSG time constant τ_d, and the following equation (15). In this way, the PLL operation is achieved with the designated phase margin value.

$$PM = a\tan\left(\frac{b^2-1}{2b}\right) \tag{14}$$

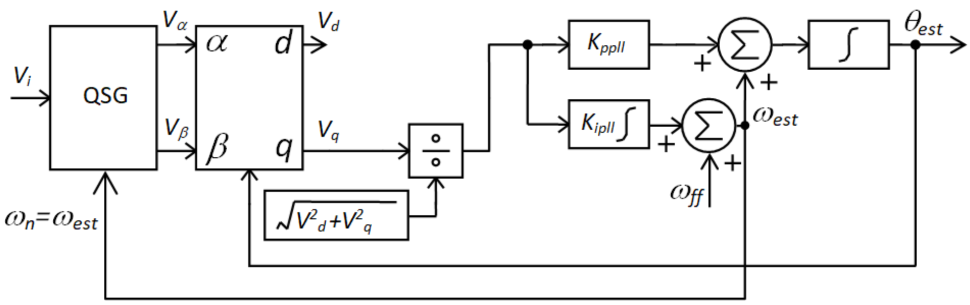

Figure 14. Conventional single phase PLL scheme [1] with QSG

$$\omega_c = \frac{1}{\tau_d b} \tag{15}$$

The PLL parameters are derived by using (16) and (17).

$$K_{ppll} = \omega_c \tag{16}$$

$$K_{ipll} = \frac{\omega_c^2}{b} \tag{17}$$

Based on the simulation results in Section IV the time constants of all four examined QSG algorithms can be approximated by $\tau_d \approx 10$ ms, which based on (16) and (17) results in K_{ppll} = 47.6 and K_{ipll} = 941. The PLL input signal frequency value is set to ω_n = 314 rad/s.

Also, in this subsection the higher harmonics are added to the PLL input signal, which correspond to the following formula (18), for the PLL input main harmonic with the amplitude equal to 1.

$$\underline{V_h} = V_{h\alpha} + jV_{h\beta} = \frac{e^{jh\omega t}}{2h}, h \in [2,13] \tag{18}$$

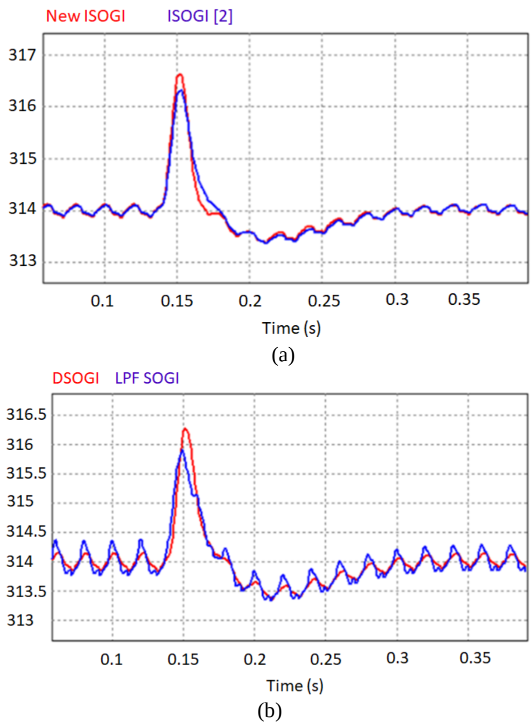

Figure 15. PLL output ω_{est} for input signal DC offset step variations, for (a) the new ISOGI and ISOGI [2], and (b) for DSOGI and SOGI with LPF

By analysing traces in Fig. 15, the following settling times (ω_{est}) are obtained: (i) for new ISOGI, t_{set} = 160 ms, (ii) for ISOGI [2], t_{set} = 190 ms, (iii) for DSOGI, t_{set} = 280 ms and (iv) for SOGI with LPF, t_{set} = 200 ms. Based on the outlined results, it can be concluded that the single phase-locked loops, operating with same parameters for four different QSG implementations, have the fastest settling time with the ISOGI tuned by the new QSG parameter tuning procedure.

C. Phase-locked Loop with Different QSG Algorithms, for the Input Signal Frequency Variations

In this subsection, the PLL performance is analyzed for four examined QSG methods, for the single phase PLL input signal frequency, varying in the range $\omega_n \in$ [314 rad/s, 344 rad/s], for K_{ppll} = 64 and K_{ipll} =65.6.

In this way the new tuning procedure is compared under equal experimental conditions for four different PLL cases.

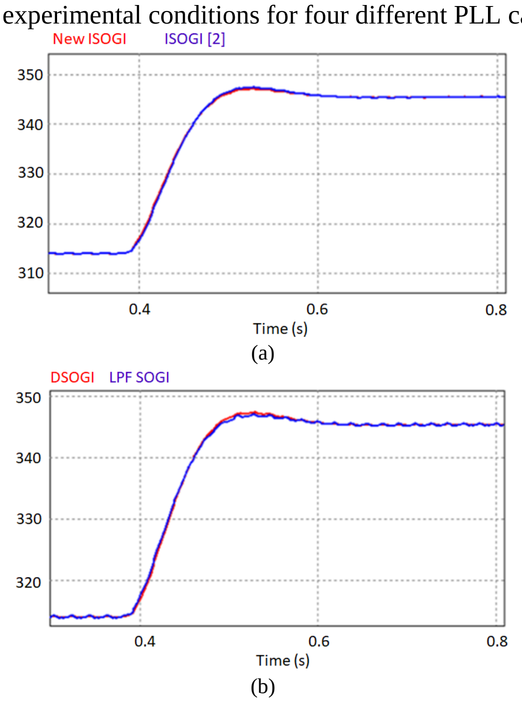

Figure 16. PLL output ω_{est} for input signal frequency variations in the range [314 rad/s, 344 rad/s], for (a) the new ISOGI and ISOGI [2], and (b) for DSOGI and SOGI with LPF

Based on the outlined experimental results presented in subsections A, B and C, it can be concluded that the ISOGI, tuned by the new parameter tuning procedure, enables the fastest settling times, when compared to ISOGI [2], DSOGI and SOGI with LPF based DC offset compensation.

VII. Conclusions

In this paper, the modified ISOGI parameter tuning procedure is presented, which is used in the SOGI applications with the input DC offset compensation based on the additional integral term. Namely, there are three conventional techniques that are used for this purpose– DSOGI, SOGI with LPF and ISOGI with the parameter tuning procedure outlined in the previous research [2]. Of these three algorithms, DSOGI is the most complex to implement, while SOGI with LPF is sensitive in relation to the employed LPF bandwidth. Finally, the ISOGI represents the simplest solution that can enable SOGI dynamic performance, similar to or better then DSOGI and SOGI with LPF. However, the existing ISOGI parameter tuning procedure is not defined in the strict algorithmic manner, but as an empirical procedure based on the trial-and-error parameter tuning [2]. To improve on this ISOGI shortcoming, the novel parameter tuning procedure is outlined in this paper, which establishes a relationship between the required dominant QSG filter closed-loop poles frequency value and ISOGI parameter values. The novel ISOGI parameter tuning procedure is compared with the conventional algorithms by both simulation and experimental tests. The most similar solution is represented by ISOGI based single-phase PLL outlined in [2], which is improved in this paper by introducing modified closed-loop PLL pole-placement technique, based on the designated closed-loop conjugate poles damping factor value. The simulation and experimental test results outlined in Sections IV and VI show that the novel tuning procedure improves the ISOGI procedure from the previous study [2], by enabling the faster settling times and more comprehensive and simpler tuning algorithm.

REFERENCES

[1] M. Xie, H. Wen, C. Zhu, and Y. Yang, "DC offset rejection improvement in single-phase SOGI-PLL algorithms: Methods review and experimental evaluation," IEEE Access, vol. 5, pp. 12810-12819, 2017. doi:10.1109/ACCESS.2017.2719721

[2] M. Karimi-Ghartemani, S. A. Khajehoddin, P. K. Jain, A. Bakhshai, and M. Mojiri, "Addressing DC component in PLL and notch filter algorithms," IEEE Transactions on Power Electronics, vol. 27, pp. 78-86, 2012. doi:10.1109/TPEL.2011.2158238

[3] S. Golestan, J. M. Guerrero, and G. B. Gharehpetian, "Five approaches to deal with problem of DC offset in phase-locked loop algorithms: Design considerations and performance evaluations," IEEE Transactions on Power Electronics, vol. 31, pp. 648-661, 2016. doi:10.1109/tpel.2015.2408113

[4] S. Golestan, J. M. Guerrero, and J. C. Vasquez, "Three-phase PLLs: A review of recent advances," IEEE Transactions on Power Electronics, vol. 32, pp. 1894-1907, 2017. doi:10.1109/TPEL.2016.2565642

[5] S. Golestan, J. M. Guerrero, and J. C. Vasquez, "Single-phase PLLs: A review of recent advances," IEEE Transactions on Power Electronics, vol. 32, pp. 9013-9030, 2017. doi:10.1109/TPEL.2017.2653861

[6] Y. Han, M. Luo, X. Zhao, J. M. Guerrero, and L. Xu, "Comparative performance evaluation of orthogonal-signal-generators-based single-phase PLL algorithms - A survey," IEEE Transactions on Power Electronics, vol. 31, pp. 3932-3944, 2016. doi:10.1109/TPEL.2015.2466631

[7] X. Huang, L. Dong, F. Xiao, and X. Liao, "A new orthogonal signal generator with DC offset rejection for single-phase phase locked loops," Journal of Power Electronics, vol. 16, pp. 310-318, 2016. doi:10.6113/JPE.2016.16.1.310

[8] C. Zhang, X. Zhao, X. Wang, X. Chai, Z. Zhang, and X. Guo, "A grid synchronisation PLL method based on mixed second-and third-order generalised integrator for DC-offset elimination and frequency adaptability," IEEE Journal of Emerging and Selected Topics in Power Electronics, vol. 6, no. 3, pp. 1517-1526, 2018. doi:10.1109/JESTPE.2018.2810499

[9] Z. Xin, X. Wang, Z. Qin, M. Lu, P. C. Loh, and F. Blaabjerg, "An improved second-order generalised integrator based quadrature signal generator," IEEE Transactions on Power Electronics, vol. 31, pp. 8068-8073, 2016. doi:10.1109/TPEL.2016.2576644

[10] S. Golestan, S. Y. Mousazadeh, J. M. Guerrero, and J. C. Vasquez, "A critical examination of frequency-fixed second-order generalised integrator-based phase-locked loops," IEEE Transactions on Power Electronics, vol. 32, pp. 6666-6672, 2017. doi:10.1109/TPEL.2017.2674973

[11] P. Kanjiya, V. M. Khadkikar, and M. S. ElMoursi, "Adaptive low-pass filter based DC offset removal technique for three-phase PLLs," IEEE Transactions on Industrial Electronics, vol. 65, no. 11, pp. 9025 - 9029, 2018. doi:10.1109/TIE.2018.2814015

[12] T. Ngo, Q. Nguyen, and S. Santoso, "Improving performance of single-phase SOGI-FLL under DC-offset voltage condition," in Industrial Electronics Society, IECON 2014-40th Annual Conference of the IEEE, 2014, pp. 1537-1541. doi:10.1109/IECON.2014.7048706

[13] M. Ciobotaru, R. Teodorescu, and V. G. Agelidis, "Offset rejection for PLL based synchronisation in grid-connected converters," in Applied Power Electronics Conference and Exposition, 2008. APEC 2008. Twenty-Third Annual IEEE, 2008, pp. 1611-1617. doi:10.1109/APEC.2008.4522940

[14] A. Kulkarni and V. John, "Design of a fast response time single-phase PLL with dc offset rejection capability," Electric Power Systems Research, vol. 145, pp. 35-43, 2017. doi:10.1016/j.epsr.2016.12.023

[15] K. J. Astrom and R. M. Murray, Feedback systems: An introduction for scientists and engineers. Princeton University press, 2010. doi:10.1515/9781400828739

[16] S. Golestan, M. Monfared, F. D. Freijedo, and J. M. Guerrero, "Dynamics assessment of advanced single-phase PLL structures," IEEE Transactions on Industrial Electronics, vol. 60, pp. 2167-2177, 2013. doi:10.1109/TIE.2012.2193863

[17] G. S., Guerrero, J. M., and G. B. Gharehpetian, "Five approaches to deal with problem of DC offset in phase-locked loop algorithms: Design considerations and performance evaluations," IEEE Transactions on Power Electronics, vol. 31, pp. 648-661, 2016. doi:10.1109/tpel.2015.2408113

[18] G. Saeed, J. M. Guerrero, and J. C. Vasquez, "DC-offset rejection in phase-locked loops: A novel approach," IEEE Transactions on Industrial Electronics, vol. 63, no. 8, pp. 4942-4946, 2016. doi:10.1109/tpel.2015.2408113

[19] H., Nanmu, D. Wang, and Y. Li, "A novel hybrid filter-based PLL to eliminate effect of input harmonics and DC offset," IEEE Access, vol. 6, pp. 19762-19773, 2018. doi:10.1109/ACCESS.2018.2821704

[20] A., Zunaib, N. Christofides, L. Hadjidemetriou, and E. Kyriakides, "Design of an advanced PLL for accurate phase angle extraction under grid voltage HIHs and DC offset," IET Power Electronics, vol. 11, no. 6, pp. 995-1008, 2017. doi:10.1049/iet-pel.2017.0424

[21] T. Quoc Nam, P. Wang, Y. Tang, L. Hai Koh, and F. Hoong Choo, "Compensation of DC offset and scaling errors in voltage and current measurements of three-phase AC/DC converters," IEEE Transactions on Power Electronics, vol. 33, no. 6, pp. 5401-5414, 2017. doi:10.1109/TPEL.2017.2734809

[22] Li, Yunlu, Dazhi Wang, Yi Ning, and Nanmu Hui, "DC-offset elimination method for grid synchronization," Electronics Letters, vol. 53, no. 5, pp. 335-337, 2017. doi:10.1109/JESTPE.2018.2810499

[23] B. Yu, X. Guo, B. Wang, and Y. Li, "Fully digital grid synchronization under harmonics and unbalanced conditions," IEEE Access, no. 7, pp. 109969-109981, 2019. doi:10.1109/access.2019.2933564

[24] T. Quoc Nam, P. Wang, and F. Hoong Choo, "An improved control strategy of three-phase PWM rectifiers under input voltage distortions and DC-offset measurement errors," IEEE Journal of Emerging and Selected Topics in Power Electronics, vol. 5, no. 3, pp. 1164-1176, 2017. doi:10.1109/JESTPE.2017.2670229

[25] K. Abdelhammid, A. Chouder, A. Bendib, K. Kara, and S. Barkat, "Enhanced structure of second-order generalized integrator frequency-locked loop suitable for DC-offset rejection in single-phase systems," Electric Power Systems Research, vol. 170, pp. 348-357, 2019. doi:10.1016/j.epsr.2019.01.029

[26] S. Preitl and R.-E. Precup, "An extension of tuning relations after Symmetrical Optimum method for PI and PID controllers," Automatica, vol. 35, no. 10, pp. 1731-1736, Oct. 1999. doi:10.1016/S0005-1098(99)00091-6.

[27] H. Tamas, L. Kovacs, R.-E. Precup, S. Preitl, B. Benyo, and Z. Benyo, "Cascade control for telerobotic systems serving space medicine," IFAC Proceedings, vol. 44, no. 1, 2011, pp. 3759-3764. doi:10.3182/20110828-6-IT-1002.02482